IOP Publishing *Environ. Res. Lett.* **16** (2021) 104032 https://doi.org/10.1088/1748-9326/ac263b

ENVIRONMENTAL RESEARCH
LETTERS

CrossMark

OPEN ACCESS

RECEIVED
29 May 2021

REVISED
4 September 2021

ACCEPTED FOR PUBLICATION
13 September 2021

PUBLISHED
6 October 2021

LETTER

Estimating ecosystem maximum light use efficiency based on the water use efficiency principle

Rong Gan[1,2,3], Lu Zhang[3], Yuting Yang[1], Enli Wang[4], William Woodgate[5], Yongqiang Zhang[6,*], Vanessa Haverd[7,9], Dongdong Kong[8], Tony Fischer[4], Francis Chiew[3] and Qiang Yu[6,*]

[1] State Key Laboratory of Hydroscience and Engineering, Department of Hydraulic Engineering, Tsinghua University, Beijing 100084, People's Republic of China
[2] School of Life Sciences, University of Technology Sydney, Sydney, NSW 2007, Australia
[3] CSIRO, Land and Water, GPO BOX 1700, Acton 2601, Canberra, Australia
[4] CSIRO, Agriculture and Food, GPO BOX 1700, Acton 2601, Canberra, Australia
[5] School of Earth and Environmental Sciences, The University of Queensland, Brisbane, QLD 4067, Australia
[6] Institute of Geographic Sciences and Natural Resources Research, Chinese Academy of Sciences, Beijing 100101, People's Republic of China
[7] CSIRO, Oceans and Atmosphere, GPO BOX 1700, Acton 2601, Canberra, Australia
[8] Department of Atmospheric Science, School of Environmental Studies, China University of Geosciences, Wuhan 430078, People's Republic of China
[9] The author Dr Vanessa Haverd is deceased.
* Authors to whom any correspondence should be addressed.

E-mail: zhangyq@igsnrr.ac.cn **and** yuq@nwafu.edu.cn

Keywords: maximum light use efficiency, water use efficiency, carbon, water, ecosystem

Supplementary material for this article is available online

Abstract

Light use efficiency (LUE) defines the vegetation efficiency of converting radiative energy into biochemical energy through photosynthesis. Estimating the maximum LUE ($\varepsilon_{\max}$) is critical yet challenging for quantifying gross primary production (GPP) using LUE-based models. This study describes an analytical method for estimating $\varepsilon_{\max}$ based on water use efficiency (WUE) as determined by plant water use and carbon gain. Unlike other complex parameterization schemes, this WUE-based method is simple and requires four variables relatively easy to acquire. The WUE-based $\varepsilon_{\max}$ estimates compare favorably well with values based on traditional curve fitting method and that reported in the literature, and clearly distinguished $\varepsilon_{\max}$ between C_3 (1.48 ± 0.33 g C MJ^{-1} PAR) and C_4 (2.63 ± 0.21 g C MJ^{-1} PAR) dominated ecosystems. The range in $\varepsilon_{\max}$ estimates was narrow across different years and sites within a biome. The WUE-based $\varepsilon_{\max}$ estimate is theoretically constrained by vegetation water use and can be directly incorporated into LUE models for GPP estimation across ecosystems.

1. Introduction

Vegetation converts solar energy into biochemical energy stored in carbohydrates through photosynthesis. At the ecosystem level, the efficiency of this process can be quantified as the ratio of gross primary production (GPP) to photosynthetically active radiation (PAR), commonly known as light use efficiency (LUE) (Monteith 1972, 1977). The theoretical maximum value of LUE ($\varepsilon_{\max}$) under optimal state (Bolton and Hall 1991) is usually downregulated due to biophysical and environmental constraints to obtain the actual amount of carbon assimilation, i.e. $\varepsilon_{\max} = \mathrm{GPP}/(\mathrm{PAR}{\cdot}f_{\mathrm{APAR}}{\cdot}f_s)$, where f_{APAR} is the fraction of absorbed PAR determined by light conditions and canopy properties, and f_s is the environmental stress factor representing limits induced by temperature, availability of resources, e.g. water and nutrient (Monteith 1972). This is a practical and widely adopted conceptual framework for GPP estimation across spatiotemporal scales (Potter *et al* 1993, Landsberg and Waring 1997, Veroustraete *et al* 2002, Running *et al* 2004, Xiao *et al* 2004, Yuan *et al* 2007, Yang *et al* 2013). The accuracy of such GPP models, however, relies heavily on the parameterization of $\varepsilon_{\max}$ (Cramer *et al* 1999, Ruimy *et al* 1999, Wei *et al* 2017a).

Previously studies have shown that $\varepsilon_{\max}$ values can vary by a factor of five based on experimental evidence (Choudhury 2000, Gitelson and Gamon 2015). Early studies conducted by Monteith (1977, 1986) suggested an average $\varepsilon_{\max}$ of about 1.5 g C MJ^{-1} for C_3 plants and 2.4 g C MJ^{-1} for C_4 plants. However, others found $\varepsilon_{\max}$ values vary greatly from 0.24 to 4.82 g C MJ^{-1} for various plant types (Prince 1991). Consequently, discussions have centered on whether $\varepsilon_{\max}$ is a consistent or variable parameter across species and biomes with different physical environments (Field 1991, Prince 1991, Ruimy *et al* 1994, Medlyn 1998, Kergoat *et al* 2008, Gitelson *et al* 2018, Zhang *et al* 2018). While consistent $\varepsilon_{\max}$ is often interpreted as a result of an evolutionary plant response to resource availability (Monteith 1977, Field 1991, Gitelson *et al* 2018), evidence on the contrary can be explained by biotic and abiotic factors attributed to plant or ecosystem types (Gallagher and Biscoe 1978, Prince 1991, Landsberg and Waring 1997, Sinclair and Muchow 1999, Albrizio and Steduto 2005), light quality (Choudhury 2000, Wang *et al* 2018), water (Passioura 1982, Shi *et al* 2014), nitrogen (Sinclair and Horie 1989, Kergoat *et al* 2008) and atmospheric CO_2 concentration (Dewar *et al* 1998, Norby *et al* 2003) conditions, from both experimental and theoretical perspectives (Ruimy *et al* 1994, Medlyn 1998). It is important to understand how $\varepsilon_{\max}$ varies across different species (i.e. C_3 and C_4) and biomes (e.g. forests to grasslands (GRAs)) to allow more robust estimation of GPP (Prince 1991, Gitelson and Gamon 2015, Wohlfahrt and Gu 2015).

Various methods have been used to estimate $\varepsilon_{\max}$ and they fall into two broad categories: (a) fitting light response curves (LRCs) and (b) inverting the LUE model (i.e. $\varepsilon_{\max} = \mathrm{GPP}/(\mathrm{PAR}\cdot f_{\mathrm{APAR}}\cdot f_s)$). In the first category, $\varepsilon_{\max}$ is a parameter based on the Michaelis–Menten LRC fitted to observed GPP and PAR data (Wang *et al* 2010, He *et al* 2014, Wei *et al* 2017a). The estimation is largely determined by the choice of either a linear or nonlinear model, with results varying by a factor of two (Ruimy *et al* 1995). The second is the most commonly used approach (Chen *et al* 2011, Sánchez *et al* 2015, Gitelson *et al* 2018), where $\varepsilon_{\max}$ estimation relies on the parameterization of f_{APAR} and f_s for a given GPP and PAR using the LUE framework. Specifically, f_{APAR} partitions available energy to vegetated and soil surfaces, and is usually derived from vegetation index (VI) (Mu *et al* 2007) and/or Beer's law using VI and light extinction coefficient (k_{PAR}) (Yuan *et al* 2010). f_s is a multiplicative limiting factor varying from 0 to 1 to account for temperature, water (soil and atmospheric), and nutrient conditions. On an ecosystem scale, $\varepsilon_{\max}$ can be calibrated against GPP using various schemes of f_{APAR} and f_s, often with (a) remotely sensed VI images (e.g. leaf area index (LAI), normalized difference vegetation index (NDVI) and enhanced vegetation index (EVI)) scaled to match flux site footprint (Li *et al* 2012, Yuan *et al* 2014) independently or in combination with constant k_{PAR} (Zheng *et al* 2018), and with (b) f_s as a multiplied limiting factor, based on water, temperature, and other limiting variables obtained *in-situ* or from remotely sensed data (Yuan *et al* 2007). Although this approach of employing VI and f_s to estimate $\varepsilon_{\max}$ is practical, main challenges remain to be overcome. First, there is a spatiotemporal discrepancy between the footprint of flux measurements (typically half-hourly, less than 1–3 km^2) (Chen *et al* 2012) and that of remotely sensed VIs (typically eight+ days, 10^1–10^2 km^2) (Chen *et al* 2008, Fu *et al* 2014). Second, k_{PAR} is not invariant, as it varies with canopy properties, seasonality, and vegetation type (Woodgate *et al* 2015, Zheng *et al* 2018). Therefore, f_{PAR} can be biased when it is calculated from the remotely sensed VIs and/or constant k_{PAR}, and may not accurately represent local vegetation profile. Third, the use of the multiplied limiting factor f_s can be ambiguous. For example, soil moisture, vapor pressure deficit, and temperature are widely acknowledged as covariant variables, yet they are often multiplied as independent factors to formulate f_s (Yang *et al* 2013). Additionally, the scale discrepancy similar to VIs also applies to f_s when the limiting factors are obtained from remote sensing images. Thus, difficulties and uncertainties still remain in quantifying f as a combination of VIs (with/without k_{PAR}) and f_s. Not surprisingly, a wide range of $\varepsilon_{\max}$ values have been reported across species (e.g. C_3 to C_4) and biomes (e.g. forests to GRAs). This variability further introduces high uncertainties into model-derived GPP estimates, leading to difficulties for multi-model and multi-scale assessments (Ruimy *et al* 1999, Chen *et al* 2011, Yuan *et al* 2014, Zheng *et al* 2018). These challenges highlight the need for a better understanding of this parameter and a more robust method for $\varepsilon_{\max}$ estimation.

The objectives of this study were to develop a new method for estimating $\varepsilon_{\max}$ that does not depend on the stress factor f, and to characterize the variability of $\varepsilon_{\max}$ across different species and biomes. For the first objective, we derived and tested a simple method for estimating $\varepsilon_{\max}$ from a coupled water and carbon perspective based on the water use efficiency (WUE) principle. For the second objective, we evaluated and characterized the variation of $\varepsilon_{\max}$ at globally distributed eddy covariance flux sites for typical C_3 and C_4 species as well as major biome types. We also compared our WUE-based $\varepsilon_{\max}$ estimates to that of traditional LRC fitting methods (supplementary, text S1 (available online at stacks.iop.org/ERL/16/104032/mmedia)). Our results can be implemented into GPP models that are based on the LUE framework and will be useful to inform uncertainties in GPP simulations.

2. Materials and methods

2.1. Derivation of LUE from the WUE principle

The intrinsic coupling of carbon uptake and water loss through vegetation stomata is commonly quantified by WUE, which is the ratio of actual CO_2 assimilation (A) to transpiration (T). For modeling purpose, A and T are usually assumed to reach their theoretical maximum, as potential assimilation (PA) and potential transpiration (PT), respectively when they are not subject to resources constraints (i.e. soil water availability) (Hanks 1974). The relationship between actual and PA and PT has been extensively used in biomass prediction (Ritchie 1983, Monteith 1986, Sinclair and Horie 1989), as often given in the following form (de Wit 1958, Hanks 1974, 1983, Stewart *et al* 1977, Monteith 1986)

$$\frac{A}{\mathrm{PA}} = \frac{T}{\mathrm{PT}} \tag{1}$$

where A and PA share the unit $\mathrm{g\,C\,m^{-2}\,d^{-1}}$, T and PT share the unit $\mathrm{mm\,d^{-1}}$.

Above empirical relationship implies the assumption that a fractional change in assimilation is associated with a corresponding fractional change in transpiration, due to simultaneous stomatal control on both carbon and water fluxes (Monteith 1988). By rearranging equation (1), we can obtain an explicit expression of WUE as follows

$$\mathrm{WUE} = \frac{A}{T} = \frac{\mathrm{PA}}{\mathrm{PT}}. \tag{2}$$

In order to derive $\varepsilon_{\max}$ from this equation, a straightforward method is to express PA by applying the LUE framework using $\varepsilon_{\max}$. Specifically, the PA rate under non-stressed condition for a certain canopy can be calculated as

$$\mathrm{PA} = \varepsilon_{\max}\,\mathrm{PAR}\,f_{\mathrm{APAR}} \tag{3}$$

where PAR is photosynthetic active radiation ($\mathrm{MJ\,m^{-2}\,d^{-1}}$), $\varepsilon_{\max}$ is maximum LUE ($\mathrm{g\,C\,MJ^{-1}}$ PAR), and f_{APAR} is the fraction of PAR that is intercepted by the canopy. For simplicity and consistency, PAR here is defined as the proportion of incident shortwave radiation (R_s) that falls into the 400–700 nm waveband, which is approximated as $0.45 \times R_s$ throughout this study (Monteith 1972, Britton and Dodd 1976).

Additionally, for the PA/PT term in equation (2), we assumed that the denominator PT for a given canopy could be approximated from potential evapotranspiration (PET) by attributing total PET to the vegetated area (Impens and Lemeur 1969, Childs *et al* 1977, Brisson *et al* 1993, Guan and Wilson 2009). Therefore, we have

$$\mathrm{PT} = \mathrm{PET}\,f_{\mathrm{R_n}} \tag{4}$$

where f_{Rn} is the fraction of net radiation (R_{n}) absorbed by the canopy (detailed elaboration of equation (4) is referred to text S2, supplementary). We further assumed that the fraction of intercepted PAR approximates the fraction of intercepted R_{n} over the same canopy, i.e. $f_{\mathrm{APAR}} = f_{\mathrm{Rn}}$ (see text S3, supplementary). Therefore, we have

$$\mathrm{PT} = \mathrm{PET}\,f_{\mathrm{APAR}}. \tag{4a}$$

By substituting equation (3) and equation (4*a*) to equation (2), we have:

$$\frac{A}{T} = \frac{\varepsilon_{\max}\,\mathrm{PAR}}{\mathrm{PET}}. \tag{5}$$

To obtain $\varepsilon_{\max}$, we simply rearranged equation (5) as

$$\varepsilon_{\max} = \frac{A \cdot \mathrm{PET}}{T \cdot \mathrm{PAR}} \tag{6}$$

$$\text{or } \varepsilon_{\max} = \mathrm{WUE}\,\frac{\mathrm{PET}}{\mathrm{PAR}} = \frac{A}{\mathrm{PAR}} \cdot \frac{1}{T/\mathrm{PET}}. \tag{6a}$$

Equation (6) shows that $\varepsilon_{\max}$ is linearly related to actual assimilation and transpiration (or WUE, equation (6*a*)) and is dependent on radiation (PAR) and atmospheric water demand (PET). This equation does not require additional information such as canopy profile (VIs, k_{PAR}), and environmental stress factors (f_s), or other variables needed by the LUE framework to parameterize f at flux sites. Alternatively, T/PET can be interpreted as f (equation (6*a*)), which corresponds to the effective fraction of PAR that is ultimately converted to biochemical energy stored in A. At an ecosystem scale, the use of T/PET is advantageous as it avoids the difficulty and uncertainty of calculating f_{APAR} based on k_{PAR} (fitted parameter with ambiguous mechanism) and VIs (e.g. NDVI, EVI, LAI) as well as f_s (e.g. temperature, water, nutrient) derived from observational and/or remote sensing techniques as illustrated in section 1.

Among the four variables required in equation (6), PET and PAR are relatively easy to obtain from readily available meteorological measurements at flux sites. PAR can be calculated from R_s observations. As for PET, we adopted the radiation-based Priestley–Taylor equation (Priestley and Taylor 1972), which is one of the most widely used methods to account for atmospheric water demand in hydrological and land surface modeling (Berg *et al* 2016, Maes *et al* 2019, Pagán *et al* 2019). Additionally, since A can be reasonably approximated by GPP at an ecosystem level, the only variable required to apply equation (6) is transpiration (T). It is widely acknowledged that T is difficult to measure directly and its simulation exhibits high uncertainties and large discrepancies based on the choice of methods (Wang *et al* 2014, Medlyn *et al* 2017, Wei *et al* 2017b, Zhou *et al* 2018). However, evapotranspiration (ET) can be easily derived from latent heat flux observations and can be used as a reasonable approximation of T under certain conditions (Knauer *et al* 2018, Zhou *et al* 2018). In this study we adopted the common assumption that ET is a reasonable approximation of T under conditions of high vegetation coverage and negligible soil evaporation during rain-free periods. Consequently, equation (6) becomes

$$\varepsilon_{\max} = \frac{\mathrm{GPP} \cdot \mathrm{PET}}{\mathrm{ET} \cdot \mathrm{PAR}}. \tag{7}$$

As a result, $\varepsilon_{\max}$ can be estimated from GPP, ET, PAR and PET. For practical purposes, $\varepsilon_{\max}$ can be estimated as the slope of the linear regression between GPP·PET and ET·PAR. This method for $\varepsilon_{\max}$ estimation is herein referred to as the WUE-based method in the following discussions.

2.2. FLUXNET data and VI

To test the WUE-based method proposed for determining $\varepsilon_{\max}$, meteorological and eddy covariance measurements at 52 flux sites (318 site-years of observation) were obtained from the FLUXNET database (http://fluxnet.fluxdata.org/). A brief description of the selected sites is presented in table S1 and figure S1. Half-hourly observations of latent heat flux (LE W m^{-2}), R_n (W m^{-2}), R_s (W m^{-2}) and air temperature (T_a °C) were used. Estimates of GPP derived from night time partitioning algorithm provided by FLUXNET were adopted as GPP observations in this study. PET was calculated from the Priestley–Taylor equation with the multiplication factor α_{PT} set to 1.26 (Priestley and Taylor 1972). As stated earlier, PAR was taken as 45% of the total R_s. The flux sites used in this study included seven plant functional types (PFTs) where high vegetation coverage was observed during the growing season, including evergreen broadleaf forest (EBF), deciduous broadleaf forest (DBF), evergreen needle leaf forest (ENF), GRA, woody savanna (WSA), wetland (WET) and cropland (CRO). Three crop sites with annual soybean (*Glycine max* L.) (C_3) and maize (*Zea mays* L.) (C_4) rotation were selected to represent C_3 and C_4 species in order to determine the effect of different photosynthetic pathways on $\varepsilon_{\max}$.

Original half-hourly data were filtered to retrieve reliable observations according to the standard quality control protocols (Reichstein *et al* 2005). Following criteria were used to further screening available data for $\varepsilon_{\max}$ estimation: (a) only daytime observations with R_s greater than 20 W m^{-2} were used; (b) negative entries of LE and GPP were eliminated; (c) data on rainy days (rainfall >0.5 mm) and the subsequent two days were excluded to focus only on transpiration (Beer *et al* 2009, Knauer *et al* 2018); (d) only growing season dates with high vegetation coverage present were used; (e) minimum of ten days of valid observations during each growing season were required for robust regression analysis. Growing season was defined according to Zhou *et al* (2014, 2016) as the days when daytime average GPP exceeded 10% of 95th percentile of daily GPP at a given site. High vegetation coverage was further ensured by high daily values of LAI in addition to GPP selection criterion. Observations during days when LAI exceeded a threshold of 2.0 were used to assure conditions where ET was a reasonable representation of T (Ritchie 1983, Zhou *et al* 2018).

At each study site, LAI was determined using remotely sensed LAI (eight-day, 500 m resolution) from MODIS (MOD15A2 product) using observations within a 1 km × 1 km cell centered on the site coordinates (Gan *et al* 2018). Original eight day LAI time series were (a) filtered according to quality flags to select reliable entries, (b) smoothed using Savitzky–Golay filter, and (c) linearly interpolated to determine daily LAI (Zhang *et al* 2019). These daily LAI time series were then used to assist data screening during the growing season at each site.

3. Results

3.1. Comparison of $\varepsilon_{\max}$ estimates for C_3 and C_4 species

Long-term site-level estimate of $\varepsilon_{\max}$ are illustrated in figures 1(a) and (b) for typical C_3 and C_4 species, respectively, at the site US-Ne2 (maize-soybean rotation, irrigated). Taking figure 1(a) as example, $\varepsilon_{\max}$ of soybean was estimated using equation (7) as the linear regression slope between GPP·PET and ET·PAR (section 2.1), using data from the soybean-grown seasons over multiple years (section 2.2). The regression was forced to pass through the origin to be consistent with the fact that both photosynthesis and transpiration approach zero when stomata are closed. A strong linear correlation was found between GPP·PET and ET·PAR, with the coefficient of determination (R^2) being 0.96 ($p < 0.001$). The long-term $\varepsilon_{\max}$ was then estimated as 1.47 g C MJ^{-1} PAR for soybean (C_3) at this site. To examine the applicability of the method for C_4 species, the same regression was performed during the maize-grown years as shown in figure 1(b). As expected, a clear difference was detected for the regression slope between soybean and maize. While exhibiting the same R^2 as soybean years, maize years presented a much higher $\varepsilon_{\max}$ value of 2.53 g C MJ^{-1} PAR.

The WUE-based method also provided comparable estimates of $\varepsilon_{\max}$ for C_3 and C_4 crops at two adjacent sites, namely US-Ne1 (continuous maize, irrigated) and US-Ne3 (maize-soybean rotation, rain-fed), with strong linear correlation ($R^2 \geqslant 0.95$) and $\varepsilon_{\max}$ estimated at 2.62 g C MJ^{-1} PAR for maize at US-Ne1 (irrigated), and 1.84 and 2.87 g C MJ^{-1} PAR for soybean and maize at US-Ne3 (rain-fed), respectively (table S1, supplementary). These estimates are reasonably close to that obtained at US-Ne2 shown in figure 1.

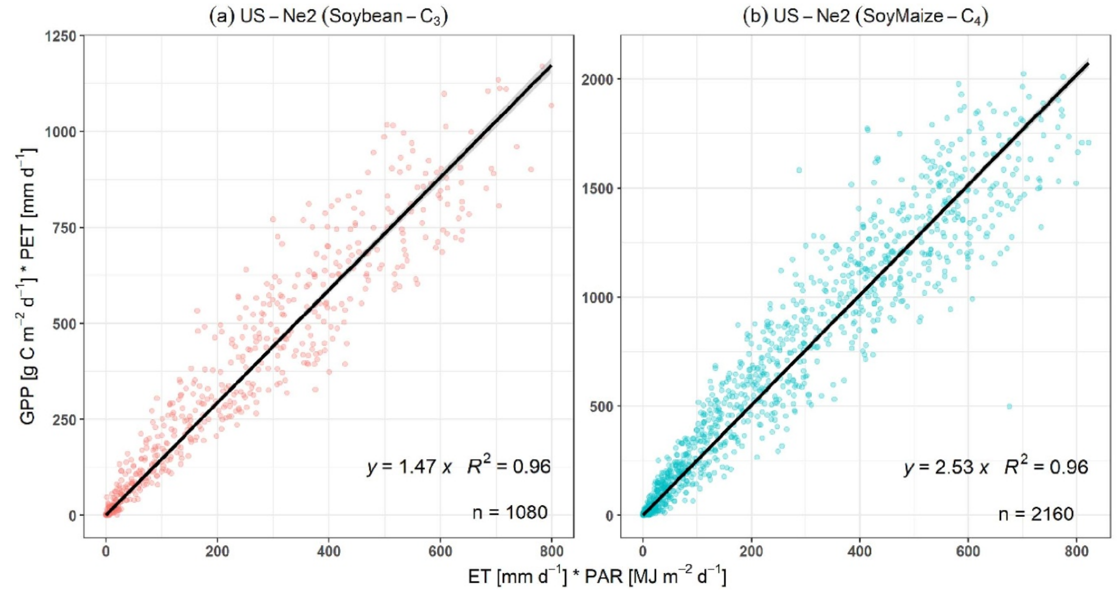

Figure 1. Comparison of ε_{max} estimate for C_3 and C_4 species at US-Ne2 (soybean grown in Nebraska, USA in 2002, 2004, 2006, and 2008 and maize grown in all other years) based on hourly observations during 2001–2012. The ε_{max} was estimated to be 1.47 g C MJ^{-1} PAR for C_3 (soybean) and 2.53 g C MJ^{-1} PAR for C_4 (maize) based on linear regression forced through the origin. '*n*' represents the number of available hourly observations at this site. The shade along each regression line represents the 95% confidence interval on the fitted values.

In comparison with the long-term estimates, the robustness of the method was further examined on an annual scale, with ε_{max} from each site-year calculated and summarized in table S2 (supplementary). For soybean, the annual average ε_{max} across US-Ne1, US-Ne2 and US-Ne3 was about 1.6 g C MJ^{-1} PAR, with a standard deviation (SD) of 0.21 g C MJ^{-1} PAR and a coefficient of variation (CV) of about 13% across six site-years. For maize, the annual mean ε_{max} was about 2.63 g C MJ^{-1} PAR, with a SD of 0.21 g C MJ^{-1} PAR and a CV of about 8% across 15 site-years. Annual average ε_{max} for maize was significantly higher than that of soybean, which agrees well with the long-term value estimated at US-Ne2. The greater ε_{max} estimates for C_4 species obtained here corresponds well with its genetically determined higher photosynthetic capacity compared with C_3 species, which demonstrates the applicability of the WUE-based method for distinguishing C_3 and C_4 dominated ecosystems.

3.2. Variation of ε_{max} across different biomes

Site-specific ε_{max} was also calculated using all available data during growing season at each of the 52 flux sites (table S1). Summary of cross-biome ε_{max} estimates are presented in figure 2. ε_{max} exhibited considerable variation within and across biome types. Among all natural ecosystems, forests (DBF, EBF, and ENF) presented a slightly higher photosynthetic capacity (greater ε_{max}) compared to non-forests (GRA, WET, and WSA). Broadleaf forests (DBF and EBF, 11 sites) with high vegetation coverage during the growing season had similar ε_{max} estimates that fell in a narrow range between 1.50 and 1.58 g C MJ^{-1} PAR. These values were in good agreement with the C_3 crop (1.66 g C MJ^{-1} PAR). ENF presented the largest variation, with ε_{max} ranging from about 0.9 to 2.4 g C MJ^{-1} PAR, and the average of 1.58 g C MJ^{-1} PAR was comparable to that of the C_3 crop. Non-forest GRA and WSA had much lower ε_{max} (less than 1.2 g C MJ^{-1} PAR on average). In addition, WETs were the least efficient in terms of light use for photosynthesis with the lowest ε_{max} of only about 0.83 g C MJ^{-1} PAR. For the four CRO sites under agricultural management (C_3 or C_4 species unspecified), ε_{max} varied from about 1.3 to 2.0 g C MJ^{-1} PAR, with an average of about 1.62 g C MJ^{-1} PAR. All natural ecosystems dominated by C_3 vegetation had much lower ε_{max} values than the C_4 crop. Although ENF and CRO had a few large values that exceeded 2.0 g C MJ^{-1} PAR, most C_3 dominant ecosystems showed ε_{max} typically lower than 2.0 g C MJ^{-1} PAR. On the contrary, ε_{max} for the C_4 crop was obviously larger than 2.4 g C MJ^{-1} PAR. These values were in good agreement with that suggested by Monteith (1977, 1986).

Annual ε_{max} was also calculated for each site-year to examine the interannual consistency of the WUE-based method and the results were summarized in table S2. The interannual variation of ε_{max} estimates are small for most biome types, as indicated by low SD and CV. The largest CV was found for ENF and WET (about 29% and 35%, respectively), and the minimum CV was found for CRO-C_4 (about 8%). Overall CV was about 20% across all C_3 dominant ecosystems. High R^2 (0.91) also provided evidence of the robustness of this method across the annual scale for different biome groups.

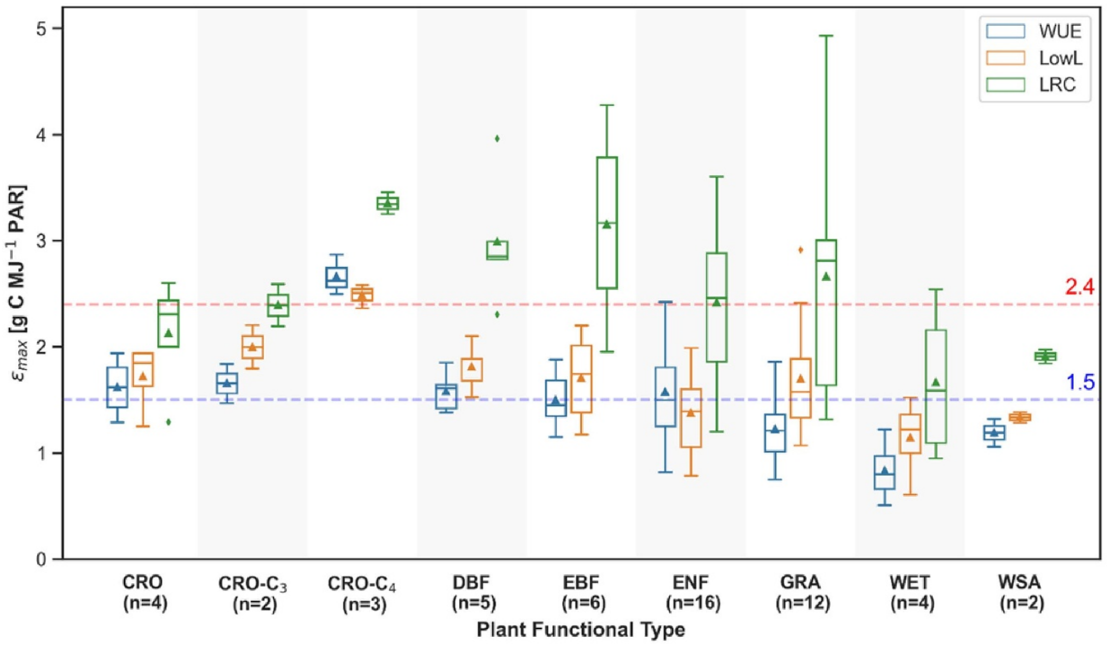

Figure 2. Biome-grouped $\varepsilon_{\max}$ estimates based on the WUE method (blue boxes) at 52 eddy covariance flux sites. For each group, the mean and median $\varepsilon_{\max}$ is shown as the triangle and the horizontal line within each box, respectively. The 25th and 75th quantiles are shown as the lower and the upper boundaries of each box, respectively. CRO-C$_3$ $\varepsilon_{\max}$ US-Ne1, US-Ne2, and US-Ne3 during soybean-grown years. CRO-C$_4$ represents $\varepsilon_{\max}$ estimates at the same sites during maize-grown years. '*n*' represents the number of flux sites within each biome group. Abbreviations for plant functional types is the same as table S1. Horizontal dash line in blue and red represents the $\varepsilon_{\max}$ value suggested by Monteith (1977, 1986) for C$_3$ and C$_4$ crops, respectively. $\varepsilon_{\max}$ estimates derived from low light regression (LowL, orange boxes) and rectangular hyperbola light response curve (LRC, green boxes) are also presented for comparison.

3.3. Comparison of $\varepsilon_{\max}$ from different methods and previous studies

In addition to the WUE-based method as proposed in this study, we also calculated $\varepsilon_{\max}$ estimates using the same dataset by fitting two traditional LRCs (text S1), as summarized in table 1 and figure 2 (details see table S1). Result show that linear LowL-based $\varepsilon_{\max}$ estimates were similar to our estimates using the WUE-based method (the differences are 0.2 g C MJ^{-1} PAR for C$_3$ and 0.18 g C MJ^{-1} PAR for C$_4$). The mean estimates are the closest for CRO whereas the largest discrepancy is found for GRA, with the difference being 0.1 and 0.47 g C MJ^{-1} PAR, respectively. Much higher $\varepsilon_{\max}$ estimates were obtained using the LRC method, which is 1.73 and 1.51 times larger than that of WUE and LowL on average. While the closest $\varepsilon_{\max}$ difference is 0.51 g C MJ^{-1} PAR for CRO, the largest difference is over 1.4 g C MJ^{-1} PAR for EBF and GRA based on LRC compared to the WUE method. It is worth noting that LRC-based $\varepsilon_{\max}$ estimates exhibit significantly higher variations (CV > 50%) across species and biomes compared to WUE (8%) and LowL (12%) method. The LRC-based $\varepsilon_{\max}$ estimates also diverse greatly from values suggested by Monteith (1977, 1986) in general. It is also noted that the R^2 values are comparable between LowL and LRC but much lower than that of the WUE method, indicating a stronger correlation between GPP·PET and ET·PAR compared to GPP and PAR (regardless of linear or non-linear regression).

Apart from LowL and LRC methods, we also compared WUE-based $\varepsilon_{\max}$ estimates to those reported in previous studies. Across species and biomes, our $\varepsilon_{\max}$ estimates agree well with the results from experimental and modeling estimates reported in the literature. For C$_3$ and C$_4$ crops at the same sites (i.e. US-Ne1, US-Ne2, and US-Ne3), Gitelson *et al* (2018) reported similar but slightly lower $\varepsilon_{\max}$ values for soybean and maize, i.e. 1.45 and 2.23 g C MJ^{-1} PAR (using green LAI and intercepted PAR measurements) compared to our estimates of 1.66 and 2.67 g C MJ^{-1} PAR, respectively (figure S2). Besides, our $\varepsilon_{\max}$ estimates were almost identical to those obtained by Nguy-Robertson *et al* (2015) at the same sites for both soybean (1.72 g C MJ^{-1} PAR) and maize (2.42 g C MJ^{-1} PAR), and comparable to that of Chen *et al* (2011) for maize (1.95 g C MJ^{-1} PAR) using optimized LUE models. Zhang *et al* (2016, 2017), suggested that $\varepsilon_{\max}$ should be less than 2 g C MJ^{-1} PAR for C$_3$ and close to 3 g C MJ^{-1} PAR for C$_4$ vegetation based on sun-induced chlorophyll fluorescence, which is also consistent with our $\varepsilon_{\max}$ estimates. These comparisons showed that the WUE-based method provides reasonable $\varepsilon_{\max}$ estimates for species with distinct photosynthetic capacity differences.

For the other biomes, the WUE-based method also produced $\varepsilon_{\max}$ estimates that were comparable to those reported in the literature (figure S4). Our WUE-based $\varepsilon_{\max}$ estimates were close to those from

Table 1. $\varepsilon_{\max}$ estimates from WUE, LowL, and LRC methods. $\varepsilon_{\max}$ for each species and biome group was calculated as cross-site averages. Coefficient of variation (CV) and coefficient of determination (R^2) are also shown.

	$\varepsilon_{\max}$			CV (%)			R^2		
PFT[a]	WUE	LowL	LRC	WUE	LowL	LRC	WUE	LowL	LRC
CRO-C_4	2.67 ± 0.19	2.49 ± 0.11	3.35 ± 0.11	3.56	1.14	1.11	0.96	0.76	0.87
CRO-C_3	1.66 ± 0.26	2.00 ± 0.29	2.39 ± 0.28	6.84	8.40	8.00	0.97	0.63	0.77
CRO	1.62 ± 0.29	1.72 ± 0.33	2.13 ± 0.58	8.35	10.64	33.37	0.95	0.70	0.76
DBF	1.58 ± 0.19	1.82 ± 0.22	2.98 ± 0.61	3.58	4.76	36.63	0.88	0.51	0.55
EBF	1.50 ± 0.27	1.70 ± 0.41	3.15 ± 0.90	7.33	17.16	80.20	0.83	0.35	0.46
ENF	1.58 ± 0.53	1.38 ± 0.35	2.42 ± 0.74	24.29	12.54	54.14	0.89	0.48	0.57
GRA	1.22 ± 0.28	1.70 ± 0.55	2.66 ± 1.15	8.06	29.80	132.21	0.91	0.53	0.63
WET	0.83 ± 0.26	1.14 ± 0.39	1.67 ± 0.75	9.08	15.14	56.19	0.89	0.35	0.67
WSA	1.19 ± 0.18	1.34 ± 0.08	1.91 ± 0.09	3.38	0.61	0.85	0.91	0.16	0.55
Average (except C_4)	1.40 ± 0.28	1.60 ± 0.33	2.41 ± 0.64	8.86	12.38	50.20	0.90	0.46	0.62

[a] PFT type is referred to table S1 for details.

the EC-LUE model across most biomes (DBF, EBF, ENF, GRA, and WSA), and also similar to the results obtained with two other models, namely MODIS and CFix reported by Yuan *et al* (2014). However, small differences were found between the WUE-based $\varepsilon_{\max}$ estimates here and the result of Yuan *et al* (2014) for broad leaf forests (DBF and EBF) when compared with other biome types on average, except for the model VPRM. Major differences for forest and crops were found when compared with other biomes from Wang *et al* (2010) and the MODIS look-up-table (Running and Zhao 2015).

For further validation, we also compared WUE-based $\varepsilon_{\max}$ to those determined from experimental studies. In the original LUE Monteith (1972, 1977) suggested a relatively consistent $\varepsilon_{\max}$ of about 1.4 g C MJ^{-1} PAR for C_3 crops. However, lower $\varepsilon_{\max}$ values that varied between 0.2 and 1.5 g C MJ^{-1} PAR were found for woody vegetation (Raymond 1994). Other experimental results presented a wider range of 0.2–4.8 g C MJ^{-1} PAR as summarized by Prince (1991). Our $\varepsilon_{\max}$ estimates fell in these broad ranges yet showed a much narrower variation between 0.83a and 1.66 g C MJ^{-1} PAR for C_3 dominated ecosystems. Interestingly, the biomass measurements conducted by Cannell *et al* (1988) estimated $\varepsilon_{\max}$ of 1.5–1.6 g C MJ^{-1} PAR for the broad-leaf forests (DBF and EBF), which is essentially the same as the WUE-based $\varepsilon_{\max}$ estimates in this study (1.5–1.58 g C MJ^{-1} PAR).

4. Discussion

4.1. Strength of WUE method for estimating $\varepsilon_{\max}$

The WUE-based method proposed in this study provides a new perspective and a coupled approach for estimating ecosystem scale $\varepsilon_{\max}$. Compared to the traditional LRC fitting method that is highly sensitive to the choice of linear or non-linear model, i.e. LRC estimated $\varepsilon_{\max}$ was 1.5 times greater than LowL accompanied by 4 times larger CV, the WUE-based method was less variant and provides more convergent $\varepsilon_{\max}$ estimates (figure 2 and table 1). Although curve fitting is straightforward and requires only GPP and PAR, previous studies had a similar issue performing parameterization especially LRC which can lead to unrealistic and variant $\varepsilon_{\max}$ estimates (Ruimy *et al* 1995, Ye 2007, Ye and Yu 2008). Compared to the LUE-reversing method, the WUE-based method requires only four variables that are relatively easy to acquire at site or on larger scales. A major limitation of deriving $\varepsilon_{\max}$ by reversing the LUE models is the consideration of water (e.g. soil moisture) as an abiotic limit for carbon assimilation (He *et al* 2014, Yuan *et al* 2014, Wagle *et al* 2016, Hu *et al* 2018), implying that limited water availability constrains carbon assimilation. The intrinsic biophysical coupling between water loss and carbon gain, however, demonstrates that the two fluxes depend on each other and constrain each other interactively (Katul *et al* 2010, Medlyn *et al* 2011). Accordingly, the energy-converting efficiency of the carbon process should be related to WUE. The WUE-based method presents this coupling relationship explicitly, where $\varepsilon_{\max}$ is a function of WUE (biophysical processes), environmental condition (atmospheric water demand, and energy availability). Therefore, the WUE-based method directly conceptualizes and presents the joint regulation of vegetation on both water and carbon processes.

Our result also demonstrates that the WUE-based method is simple and robust for $\varepsilon_{\max}$ estimation. The much higher $\varepsilon_{\max}$ for C_4 crops which have a different photosynthetic pathway than C_3 vegetation is clearly distinguishable. The method produced $\varepsilon_{\max}$ estimates for C_3 and C_4 species that were comparable with estimates based on LowL and values reported in the literature (section 3.3, figure S3). The method was also capable of producing consistent $\varepsilon_{\max}$ for different ecosystems under a wide range of climate showing good agreement with LowL and previous studies (figure S4). In principle, $\varepsilon_{\max}$ should be achieved at lower PAR, as calculated by LowL regression in this study. Hence, the relatively close $\varepsilon_{\max}$ estimates obtained by WUE compared to LowL method may be considered as a reasonable verification of the reliability of our method, whereas the large uncertainties in LRC estimates require further investigation. The differences of $\varepsilon_{\max}$ estimates based on reversing LUE model compared to WUE method (figure S4) can be partly attributed to the uncertainties when parameterizing the f factor (i.e. VIs, k_{PAR}, f_s) using different LUE models (as illustrated in section 2.1), which contains scale discrepancy and covariant limiting factor issues. Others also argued that the uncertainty in parameterizing the f factor is a major limitation of the LUE model, and can result in inconsistent estimates of $\varepsilon_{\max}$ (Yuan *et al* 2014, Zheng *et al* 2018).

The slightly wider variation of annual $\varepsilon_{\max}$ estimates for CRO at an annual scale (table S2) (CV = 22%) is likely due to possible changes in species grown within and across crop sites and years (possible C_3 and C_4 rotation), and this may require further information and investigation. For other ecosystems, the variation in the annual $\varepsilon_{\max}$ estimates were also relatively small across different sites within a PFT (SD generally <25% of the mean $\varepsilon_{\max}$). Previous studies have demonstrated that canopy characteristics (Sánchez *et al* 2015), water availability and nutrients (Christina *et al* 2015), as well as radiation conditions (Gitelson *et al* 2015, Wang *et al* 2018), could contribute to variations in $\varepsilon_{\max}$. The possible interannual variation of $\varepsilon_{\max}$ induced by such biophysical and environmental factors was explicitly presented in our method, shown by equation (6). A further analysis between the biophysical underlying WUE ($\mathrm{uWUE_a} = \mathrm{GPP{\cdot}VPD^{0.5}/ET}$, Zhou *et al* 2014) and annual $\varepsilon_{\max}$ (figure S5) showed that photosynthetic capacity co-varied with the vegetation water use and the atmospheric water demand.

Since it is difficult to obtain ground-truth measurements for such a wide range of biome types globally distributed, we can infer from the above comparisons and discussions that the WUE-based method is reliable for $\varepsilon_{\max}$ estimation in accordance with current knowledge.

4.2. Possible implication and limitation

The WUE-based $\varepsilon_{\max}$ estimates can be directly incorporated with LUE models at local to regional scales according to species and biome types for GPP estimation. With a narrow range of $\varepsilon_{\max}$ (0.83–1.62 $\mathrm{g\,C\,MJ^{-1}}$ PAR for C_3 dominated ecosystems, figure 2), uncertainty in GPP estimates is likely to be reduced using our $\varepsilon_{\max}$ values across different ecosystems (compared with other parameterization schemes, figures 2, S3–S4). Moreover, this WUE-based method uses T/PET as a top-down limiting factor instead of the ambiguous f factor in the LUE model. This treatment not only simplifies the parameterization of $\varepsilon_{\max}$, but also avoids the possible uncertainties brought about by multiplying various limiting factors (e.g. LAI, VPD, soil water, etc) to quantify f. Additionally, because all variables required by this WUE-based method are readily available at flux sites (where the GPP models are calibrated to), local $\varepsilon_{\max}$ estimates can be easily obtained with high credibility. Measurements from these flux sites are considered highly reliable and accurate as eddy covariance represents the state-of-the-art technique. As such, $\varepsilon_{\max}$ estimates using the WUE-based method are likely to be more robust than estimates from traditional methods, and the use of this method can help to assess model uncertainty in GPP estimation. This is especially true when LUE model structure and data reliability require further evaluation, while the $\varepsilon_{\max}$ value is theoretically and biophysically consistent.

A limitation of the WUE-based method for estimating $\varepsilon_{\max}$ is the assumption that transpiration (T) can be approximated by total ET under high vegetation coverage. While this assumption is valid under complete or high vegetation coverage across the landscape, T could be less than ET in non-forest ecosystems (WET, GRA, and WSA). More accurate $\varepsilon_{\max}$ estimates would be possible using transpiration measurements (rather than using ET as an approximation) based on sap flow and/or isotopic techniques (Roupsard *et al* 2006, Wang *et al* 2014, Wei *et al* 2017b). Future studies could try to employ the latest SAPFLUXNET data (Poyatos *et al* 2016) to derive *in-situ* T to be implemented in our WUE-based method. Current site-based $\varepsilon_{\max}$ could be extrapolated to regional scale via PFT look-up-table method as adopted in the MODIS GPP algorithm. For regions where reliable ET estimates are available, our method can also be used under high LAI to derive $\varepsilon_{\max}$. For simplicity, this study also assumed that the fraction of absorbed PAR is the same as that of absorbed R_n. Ross (1981) showed that both shortwave and longwave radiation can be approximated by Beer's law with the same bulk extinction coefficient k. We consider such assumption is valid for big-leaf canopy as conceptualized in this study (text S3). Variations in k can be further explored considering different canopy characteristics (e.g. leaf inclination angle, nutrient status, phenology) and climate and radiation conditions (e.g. direct and diffuse radiation, atmospheric CO_2 concentration) (Turner *et al* 2003, Dai *et al* 2004, Wang *et al* 2018). Yet such variation should not violate the fundamentals and conclusions of this study.

5. Conclusions

This study proposed a new method to estimate $\varepsilon_{\max}$ based on the water and carbon coupling principle. The method was examined at 52 flux sites across different vegetation species and biome types. Results showed that the method was capable of distinguishing vegetation types with different photosynthetic pathways. The estimated $\varepsilon_{\max}$ for seven main biomes distributed global-wide agreed well with experimental and modeling methods. The WUE-based method is simple and the $\varepsilon_{\max}$ estimates could be incorporated into LUE models for better GPP simulation. The method could also be used to better understand the behavior and variation of $\varepsilon_{\max}$ across species and biomes considering interrelated water and carbon processes.

Data availability statement

The data that support the findings of this study are openly available at the following URL/DOI: http://fluxnet.fluxdata.org/.

Acknowledgments

The authors acknowledge the FLUXNET community for sharing the free use eddy covariance data. MODIS product (MOD15A2) was provided by the Land Processes Distributed Active Archive Centre (LPDAAC). The authors thank Dr Ian Harman and Dr Ying Ping Wang for providing constructive advices. This study is financially supported by the Ministry of Science and Technology of China (Grant No. 2019YFC1510604) and the National Natural Science Foundation of China (Grant Nos. 42041004, 42071029, and 41890821). R Gan is supported by the joint scholarship of University of Technology Sydney and China Scholarship Council and the CSIRO postgraduate top-up scholarship. Y Zhang is supported by the CAS Pioneer Talents Program. The authors thank the two anonymous referees for providing valuable suggestions to improve the quality of the manuscript. The authors declare no conflict of interest.

ORCID iDs

Rong Gan https://orcid.org/0000-0002-8629-2811
Lu Zhang https://orcid.org/0000-0002-0442-5730
Yuting Yang https://orcid.org/0000-0002-4573-1929
Enli Wang https://orcid.org/0000-0002-6653-5791
William Woodgate https://orcid.org/0000-0002-5298-4828
Yongqiang Zhang https://orcid.org/0000-0002-3562-2323
Vanessa Haverd https://orcid.org/0000-0003-4359-5895
Dongdong Kong https://orcid.org/0000-0003-1836-8172
Tony Fischer https://orcid.org/0000-0002-0740-8389
Francis Chiew https://orcid.org/0000-0001-8020-8773
Qiang Yu https://orcid.org/0000-0001-6950-1821

References

Albrizio R and Steduto P 2005 Resource use efficiency of field-grown sunflower, sorghum, wheat and chickpea: I. Radiation use efficiency *Agric. For. Meteorol.* **130** 254–68

Beer C *et al* 2009 Temporal and among-site variability of inherent water use efficiency at the ecosystem level *Glob. Biogeochem. Cycles* **23** 1–13

Berg A *et al* 2016 Land-atmosphere feedbacks amplify aridity increase over land under global warming *Nat. Clim. Change* **6** 869–74

Bolton J R and Hall D O 1991 The maximum efficiency of photosynthesis *Photochem. Photobiol.* **53** 545–8

Brisson N, Olioso A and Clastre P 1993 Daily transpiration of field soybeans as related to hydraulic conductance, root distribution, soil potential and midday leaf potential *Plant Soil* **154** 227–37

Britton C M and Dodd J D 1976 Relationships of photosynthetically active radiation and shortwave irradiance *Agric. Meteorol.* **17** 1–7

Cannell M G R, Sheppard L J and Milne R 1988 Light use efficiency and woody biomass production of poplar and willow *Forestry* **61** 125–36

Chen B *et al* 2012 Characterizing spatial representativeness of flux tower eddy-covariance measurements across the Canadian Carbon Program Network using remote sensing and footprint analysis *Remote Sens. Environ.* **124** 742–55

Chen B, Chen J M, Mo G, Black T A and Worthy D E J 2008 Comparison of regional carbon flux estimates from CO_2 concentration measurements and remote sensing based footprint integration *Glob. Biogeochem. Cycles* **22** GB2012

Chen T, van der Werf G R, Dolman A J and Groenendijk M 2011 Evaluation of cropland maximum light use efficiency using eddy flux measurements in North America and Europe *Geophys. Res. Lett.* **38** 1–5

Childs S W, Gilley J R and Splinter W E 1977 A simplified model of corn growth under moisture stress *Trans. ASAE* **20** 858–65

Choudhury B J 2000 A sensitivity analysis of the radiation use efficiency for gross photosynthesis and net carbon accumulation by wheat *Agric. For. Meteorol.* **101** 217–34

Christina M, le Maire G, Battie-Laclau P, Nouvellon Y, Bouillet J P, Jourdan C, Leonardo D M G J and Laclau J P 2015 Measured and modeled interactive effects of potassium deficiency and water deficit on gross primary productivity and light-use efficiency in *Eucalyptus grandis* plantations *Glob. Change Biol.* **21** 2022–39

Cramer W *et al* (Intercomparison T P O F T P N M) 1999 Comparing global models of terrestrial net primary productivity (NPP): overview and key results *Glob. Change Biol.* **5** 1–15

Dai Y, Dickinson R E and Wang Y 2004 A two-big-leaf model for canopy temperature, photosynthesis, and stomatal conductance *J. Clim.* **17** 2281–99

de Wit C T 1958 Transpiration and crop yields *Versl. Landbouwk. Onderz.* **64** 88 (available at: https://library.wur.nl/WebQuery/wurpubs/412958)

Dewar R C, Medlyn B E and McMurtrie R E 1998 A mechanistic analysis of light and carbon use efficiencies *Plant Cell Environ.* **21** 573–88

Field C B 1991 Ecological scaling of carbon gain to stress and resource availability *Response of Plants to Multiple Stresses* and (San Diego: Academic) pp 35–65

Fu D *et al* 2014 Estimating landscape net ecosystem exchange at high spatial–temporal resolution based on Landsat data, an improved upscaling model framework, and eddy covariance flux measurements *Remote Sens. Environ.* **141** 90–104

Gallagher J N and Biscoe P V 1978 Radiation absorption, growth and yield of cereals *J. Agric. Sci.* **91** 47–60

Gan R, Zhang Y, Shi H, Yang Y, Eamus D, Cheng L, Chiew F H S and Yu Q 2018 Use of satellite leaf area index estimating evapotranspiration and gross assimilation for Australian ecosystems *Ecohydrology* **11** e1974

Gitelson A A, Arkebauer T J and Suyker A E 2018 Convergence of daily light use efficiency in irrigated and rainfed C_3 and C_4 crops *Remote Sens. Environ.* **217** 30–37

Gitelson A A and Gamon J A 2015 The need for a common basis for defining light-use efficiency: implications for productivity estimation *Remote Sens. Environ.* **156** 196–201

Gitelson A A, Peng Y, Arkebauer T J and Suyker A E 2015 Productivity, absorbed photosynthetically active radiation, and light use efficiency in crops: implications for remote sensing of crop primary production *J. Plant Physiol.* **177** 100–9

Guan H and Wilson J L 2009 A hybrid dual-source model for potential evaporation and transpiration partitioning *J. Hydrol.* **377** 405–16

Hanks R J 1974 Model for predicting plant yield as influenced by water use *Agron. J.* **66** 660–5

Hanks R J 1983 Yield and water-use relationships: an overview *Limitations to Efficient Water Use in Crop Production* (Madison, WI: American Society of Agronomy, Inc. Crop Science Society of America, Inc. Soil Science Society of America, Inc.) pp 393–411

He H *et al* 2014 Large-scale estimation and uncertainty analysis of gross primary production in Tibetan alpine grasslands *J. Geophys. Res. Biogeosci.* **119** 466–86

Hu Z *et al* 2018 Joint structural and physiological control on the interannual variation in productivity in a temperate grassland: a data-model comparison *Glob. Change. Biol.* **24** 2965–79

Impens I and Lemeur R 1969 Extinction of net radiation in different crop canopies *Arch. Meteorol. Geophys. Bioklimatol.* B **17** 403–12

Katul G, Manzoni S, Palmroth S and Oren R 2010 A stomatal optimization theory to describe the effects of atmospheric CO_2 on leaf photosynthesis and transpiration *Ann. Bot.* **105** 431–42

Kergoat L, Lafont S, Arneth A, le Dantec V and Saugier B 2008 Nitrogen controls plant canopy light-use efficiency in temperate and boreal ecosystems *J. Geophys. Res. Biogeosci.* **113** G04017

Knauer J *et al* 2018 Towards physiologically meaningful water-use efficiency estimates from eddy covariance data *Glob. Change Biol.* **24** 694–710

Landsberg J J and Waring R H 1997 A generalised model of forest productivity using simplified concepts of radiation-use efficiency, carbon balance and partitioning *For. Ecol. Manage.* **95** 209–28

Li A, Bian J, Lei G and Huang C 2012 Estimating the maximal light use efficiency for different vegetation through the CASA model combined with time-series remote sensing data and ground measurements *Remote Sens.* **4** 3857–76

Maes W H, Gentine P, Verhoest N E C and Miralles D G 2019 Potential evaporation at eddy-covariance sites across the globe *Hydrol. Earth Syst. Sci.* **23** 925–48

Medlyn B E 1998 Physiological basis of the light use efficiency model *Tree Physiol.* **18** 167–76

Medlyn B E *et al* 2017 How do leaf and ecosystem measures of water-use efficiency compare? *New Phytol.* **216** 758–70

Medlyn B E, Duursma R A, Eamus D, Ellsworth D S, Prentice I C, Barton C V M, Crous K Y, de Angelis P, Freeman M and Wingate L 2011 Reconciling the optimal and empirical approaches to modelling stomatal conductance *Glob. Change. Biol.* **17** 2134–44

Monteith J L 1972 Solar radiation and productivity in tropical ecosystems *J. Appl. Ecol.* **9** 747–66

Monteith J L 1977 Climate and the efficiency of crop production in Britain [and discussion] *Phil. Trans. R. Soc.* B **281** 277–94

Monteith J L 1986 How do crops manipulate water supply and demand? *Phil. Trans. R. Soc.* A **316** 245–259

Monteith J L 1988 Does transpiration limit the growth of vegetation or vice versa? *J. Hydrol.* **100** 57–68

Mu Q, Heinsch F A, Zhao M and Running S W 2007 Development of a global evapotranspiration algorithm based on MODIS and global meteorology data *Remote Sens. Environ.* **111** 519–36

Nguy-Robertson A, Suyker A and Xiao X 2015 Modeling gross primary production of maize and soybean croplands using light quality, temperature, water stress, and phenology *Agric. For. Meteorol.* **213** 160–72

Norby R J, Sholtis J D, Gunderson C A and Jawdy S S 2003 Leaf dynamics of a deciduous forest canopy: no response to elevated CO_2 *Oecologia* **136** 574–84

Pagán B, Maes W, Gentine P, Martens B and Miralles D 2019 Exploring the potential of satellite solar-induced fluorescence to constrain global transpiration estimates *Remote Sens.* **11** 413

Passioura J B 1982 *Water in the Soil-Plant-Atmosphere Continuum BT—Physiological Plant Ecology II: Water Relations and Carbon Assimilation* ed O L Lange, P S Nobel, C B Osmond and H Ziegler (Berlin: Springer) pp 5–33

Potter C S, Randerson J T, Field C B, Matson P A, Vitousek P M, Mooney H A and Klooster S A 1993 Terrestrial ecosystem production: a process model based on global satellite and surface data *Glob. Biogeochem. Cycles* **7** 811–41

Poyatos R, Granda V, Molowny-Horas R, Mencuccini M, Steppe K and Martínez-Vilalta J 2016 SAPFLUXNET: towards a global database of sap flow measurements *Tree Physiol.* **36** 1449–55

Priestley C H B and Taylor R J 1972 On the assessment of surface heat flux and evaporation using large-scale parameters *Monthly Weather Rev.* **100** 81–92

Prince S D 1991 A model of regional primary production for use with coarse resolution satellite data *Int. J. Remote Sens.* **12** 1313–30

Raymond Hunt E J Jr 1994 Relationship between woody biomass and PAR conversion efficiency for estimating net primary production from NDVI *Int. J. Remote Sens.* **15** 1725–30

Reichstein M *et al* 2005 On the separation of net ecosystem exchange into assimilation and ecosystem respiration: review and improved algorithm *Glob. Change Biol.* **11** 1424–39

Ritchie J T 1983 Efficient water use in crop production: discussion on the generality of relations between biomass production and evapotranspiration *Limitations to Efficient Water Use in Crop Production* (Madison, WI: American Society of Agronomy, Inc. Crop Science Society of America, Inc. Soil Science Society of America, Inc.) pp 29–44

Ross J 1981 *The Radiation Regime and Architecture of Plant Stands* vol 3 (Dordrecht: Springer) XXVII, p 391

Roupsard O *et al* 2006 Partitioning energy and evapo-transpiration above and below a tropical palm canopy *Agric. For. Meteorol.* **139** 252–68

Ruimy A, Jarvis P G, Baldocchi D D and Saugier B 1995 CO_2 fluxes over plant canopies and solar radiation: a review *Adv. Ecol. Res.* vol 26 (San Diego: Academic) pp 1–68

Ruimy A, Kergoat L and Bondeau A (Intercomparison T P O F T P N M) 1999 Comparing global models of terrestrial net primary productivity (NPP): analysis of differences in light absorption and light-use efficiency *Glob. Change Biol.* **5** 56–64

Ruimy A, Saugier B and Dedieu G 1994 Methodology for the estimation of terrestrial net primary production from remotely sensed data *J. Geophys. Res. Atmos.* **99** 5263–83

Running S W, Nemani R R, Heinsch F A, Zhao M, Reeves M and Hashimoto H 2004 A continuous satellite-derived measure of global terrestrial primary production *Bioscience* **54** 547–60

Running S W and Zhao M 2015 Daily GPP and annual NPP (MOD17A2/A3) products NASA Earth Observing System MODIS land algorithm—user's guide V3 28 (available at: www.ntsg.umt.edu/sites/ntsg.umt.edu/files/modis/MOD17UsersGuide2015_v3.pdf)

Sánchez M L, Pardo N, Pérez I A and García M A 2015 GPP and maximum light use efficiency estimates using different approaches over a rotating biodiesel crop *Agric. For. Meteorol.* **214–215** 444–55

Shi H, Li L, Eamus D, Cleverly J, Huete A, Beringer J, Yu Q, van Gorsel E and Hutley L 2014 Intrinsic climate dependency of ecosystem light and water-use-efficiencies across Australian biomes *Environ. Res. Lett.* **9** 104002

Sinclair T R and Horie T 1989 Leaf nitrogen, photosynthesis, and crop radiation use efficiency: a review *Crop Sci.* **29** 90

Sinclair T R and Muchow R C 1999 Radiation use efficiency *Advances in Agronomy* vol 65 (New York: Academic) pp 215–65

Stewart J, Hagan R, Pruitt W, Danielson R, Franklin W, Hanks R, Riley J and Jackson E 1977 Optimizing crop production through control of water and salinity levels in the soil (Utah Water Research Laboratory) Paper 67

Turner D P, Ritts W D, Cohen W B, Gower S T, Zhao M, Running S W, Wofsy S C, Urbanski S, Dunn A L and Munger J W 2003 Scaling gross primary production (GPP) over boreal and deciduous forest landscapes in support of MODIS GPP product validation *Remote Sens. Environ.* **88** 256–70

Veroustraete F, Sabbe H and Eerens H 2002 Estimation of carbon mass fluxes over Europe using the C-Fix model and Euroflux data *Remote Sens. Environ.* **83** 376–99

Wagle P, Gowda P H, Xiao X and Anup K C 2016 Parameterizing ecosystem light use efficiency and water use efficiency to estimate maize gross primary production and evapotranspiration using MODIS EVI *Agric. For. Meteorol.* **222** 87–97

Wang H, Jia G, Fu C, Feng J, Zhao T and Ma Z 2010 Deriving maximal light use efficiency from coordinated flux measurements and satellite data for regional gross primary production modeling *Remote Sens. Environ.* **114** 2248–58

Wang L, Stephen P G and Kelly K C 2014 Global synthesis of vegetation control on evapotranspiration partitioning *Geophys. Res. Lett.* **41** 6753–7

Wang S, Ibrom A, Bauer-Gottwein P and Garcia M 2018 Incorporating diffuse radiation into a light use efficiency and evapotranspiration model: an 11-year study in a high latitude deciduous forest *Agric. For. Meteorol.* **248** 479–93

Wei S, Yi C, Fang W and Hendrey G 2017a A global study of GPP focusing on light-use efficiency in a random forest regression model *Ecosphere* **8** e01724

Wei Z, Yoshimura K, Wang L, Miralles D G, Jasechko S and Lee X 2017b Revisiting the contribution of transpiration to global terrestrial evapotranspiration *Geophys. Res. Lett.* **44** 2792–801

Wohlfahrt G and Gu L 2015 The many meanings of gross photosynthesis and their implication for photosynthesis research from leaf to globe *Plant Cell Environ.* **38** 2500–7

Woodgate W, Disney M, Armston J D, Jones S D, Suarez L, Hill M J, Wilkes P, Soto-Berelov M, Haywood A and Mellor A 2015 An improved theoretical model of canopy gap probability for Leaf Area Index estimation in woody ecosystems *For. Ecol. Manage.* **358** 303–20

Xiao X, Zhang Q, Braswell B, Urbanski S, Boles S, Wofsy S, Moore B and Ojima D 2004 Modeling gross primary production of temperate deciduous broadleaf forest using satellite images and climate data *Remote Sens. Environ.* **91** 256–70

Yang Y, Shang S, Guan H and Jiang L 2013 A novel algorithm to assess gross primary production for terrestrial ecosystems from MODIS imagery *J. Geophys. Res. Biogeosci.* **118** 590–605

Ye Z 2007 A new model for relationship between irradiance and the rate of photosynthesis in *Oryza sativa Photosynthetica* **45** 637–40

Ye Z and Yu Q 2008 Comparison of new and several classical models of photosynthesis in response to irradiance *Chinese J. Plant. Ecol.* **32** 1356–61

Yuan W *et al* 2007 Deriving a light use efficiency model from eddy covariance flux data for predicting daily gross primary production across biomes *Agric. For. Meteorol.* **143** 189–207

Yuan W *et al* 2010 Global estimates of evapotranspiration and gross primary production based on MODIS and global meteorology data *Remote Sens. Environ.* **114** 1416–31

Yuan W *et al* 2014 Global comparison of light use efficiency models for simulating terrestrial vegetation gross primary production based on the LaThuile database *Agric. For. Meteorol.* **192–193** 108–20

Zhang Y *et al* 2018 Spatio-temporal convergence of maximum daily light-use efficiency based on radiation absorption by canopy chlorophyll *Geophys. Res. Lett.* **45** 3508–19

Zhang Y *et al* 2016 Consistency between sun-induced chlorophyll fluorescence and gross primary production of vegetation in North America *Remote Sens. Environ.* **183** 154–69

Zhang Y, Kong D, Gan R, Chiew F H S, McVicar T R, Zhang Q and Yang Y 2019 Coupled estimation of 500 m and 8-day resolution global evapotranspiration and gross primary production in 2002–2017 *Remote Sens. Environ.* **222** 165–82

Zhang Y, Xiao X, Wu X, Zhou S, Zhang G, Qin Y and Dong J 2017 A global moderate resolution dataset of gross primary production of vegetation for 2000–2016 *Sci. Data* **4** 170165

Zheng Y, Zhang L, Xiao J, Yuan W, Yan M, Li T and Zhang Z 2018 Sources of uncertainty in gross primary productivity simulated by light use efficiency models: model structure, parameters, input data, and spatial resolution *Agric. For. Meteorol.* **263** 242–57

Zhou S, Yu B, Huang Y and Wang G 2014 The effect of vapor pressure deficit on water use efficiency at the subdaily time scale *Geophys. Res. Lett.* **41** 5005–13

Zhou S, Yu B, Zhang Y, Huang Y and Wang G 2016 Partitioning evapotranspiration based on the concept of underlying water use efficiency *Water Resour. Res.* **52** 1160–75

Zhou S, Yu B, Zhang Y, Huang Y and Wang G 2018 Water use efficiency and evapotranspiration partitioning for three typical ecosystems in the Heihe River Basin, northwestern China *Agric. For. Meteorol.* **253–254** 261–73